Full Paper: The size of poly(benzyl ether) dendrimers with different molecular architectures was measured by small angle neutron scattering (SANS). Both polar and non-polar solvents were used to measure the effect of solvent type. The radius of gyration (R_g) of all of the dendrimers follows a scaling law of $R_g \propto M^{1/3}$ consistent with literature values of other chemically different dendrimers. The effect of solvent type on dendrimer size was minimal.

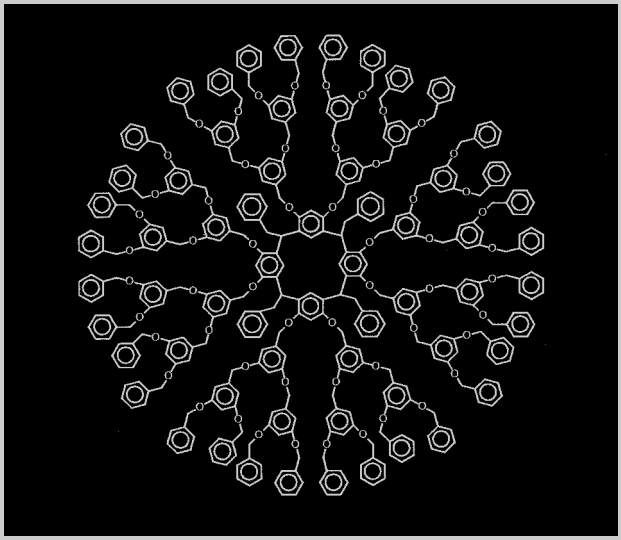

Two dimensional representation of dendritic structure for second generation of sample 150.

The Influence of Molecular Architecture and Solvent Type on the Size and Structure of Poly(benzyl ether) Dendrimers by SANS

Guennady Evmenenko,[1] *Barry J. Bauer,*[2] *Ralf Kleppinger,*[1] *Bart Forier,*[3] *Wim Dehaen,*[3] *Eric J. Amis,*[2] *Nikolai Mischenko,*[1] *Harry Reynaers**[1]

[1] Laboratory of Macromolecular Structural Chemistry, Department of Chemistry, Catholic University of Leuven, Celestijnenlaan 200F, B-3001 Heverlee, Belgium
Fax: +32-16-327990; E-mail: Harry.Reynaers@chem.kuleuven.ac.be
[2] Polymers Division, National Institute of Standards and Technology, Building 224, Room A209, Gaithersburg, Maryland 20899, USA
[3] Laboratory for Organic Synthesis, Department of Chemistry, Catholic University of Leuven, Celestijnenlaan 200F, B-3001 Heverlee, Belgium

Introduction

Dendrimers are synthetic polymeric macromolecules with a highly branched, three-dimensional architecture emanating from a central point.[1] The placement of functional groups at the polymer chain ends or in well-defined segments can determine the ultimate properties of dendritic macromolecules.[2] Because of their shape, dendrimers have very unusual physical properties. For example, dendrimers made from benzyl ether building blocks[3] have vastly different solubility from linear analogues[4] based on equivalent units, being 1.15 g/mL for the dendrimer compared to 0.025 g/mL for the analogous linear polymer in THF.

The potential use of dendrimers in a variety of technologically important applications has promoted the rapid growth of research in this field after the first dendrimer synthesis by Vögtle and co-workers 20 years ago.[5] Dendrimers are promising candidates for the future development of host-guest chemistry.[6, 7] The complex formation between dendrimers and other polymers is of practical interest in a variety of areas, such as controlled drug release systems, removal of toxic pollutants from environment, development of effective guest sensors, etc. Sugar-substituted "glyco-dendrimers"[8, 9] are also the focus of considerable research, owing to the crucial role of sugar moieties of complex carbohydrates in living systems, and the high potential of glyco-dendrimers for preventing pathogenic infections and related diseases.

Although the synthesis of dendritic materials has been extensively studied for several years, SAXS and SANS

  1022-1352/2001/0603–0891$17.50+.50/0

studies have only recently begun. Scattering techniques can be used to probe the structure of a wide range of dendrimer types in a variety of environments. There are two approaches to characterization of dendrimers through X-ray and neutron scattering methods, measurement of size variation in different solvent types, and under different ionic conditions.

The first approach is to probe the structure of dendrimers in various environments, which is essential for understanding their properties and for predicting their behavior so that a synthesis can be designed to obtain materials with predetermined properties. Up to now, only few studies have been carried out in this field. Bauer et al.[10, 11] performed SANS and SAXS experiments on poly(amido amine) (PAMAM) dendrimer aqueous solutions, and investigated the screening of the large-scale intermolecular interactions between dendrimer macromolecules upon addition of acid.

A series of carbosilane dendrimers were studied by Stark et al.[12] using X-ray scattering and quasi-elastic neutron scattering. They found that generation dependent super-structures are formed as a result of the microphase separation between the end groups and the carbosilane core. The dynamic structure factor was composed of two separable contributions referring to the segmental diffusion in the dendrimer core and the rotational diffusion of the end groups. Increasing the generation number results in slowing down the segmental diffusion and in the extension of the lifetime of local dynamical processes.

SAXS was used by Prosa et al.[13] to characterize the single-particle scattering factors produced by PAMAM and poly(propylene imine) (PPI) dendrimers. These authors presented evidence that the low generation dendrimers of the former type are less dense than their higher generation relatives; however, after a few generations ($\overline{M}_w > 50\,000$ g/mol), the average density of the dendrimers appears to be roughly independent of generation. Moreover they obtained nearly monodisperse, spherical shapes for the largest dendrimer generations with rather sharp outer boundaries.

SANS with contrast matching techniques was applied to extract the single-chain form factors of the fatty acid and the dendrimer components in bulk and dilute solution of fatty acid modified PPI dendrimers.[14] The fatty acid chains were "covalently" or "non-covalently" linked to the end groups of two generations, G3 and G5. The dendrimer core of both G3 and G5 appears to be collapsed without the incorporation of a significant amount of solvent. The same approach was used for the analysis of a dendritic structure of the fifth generation with attached diphenyl ether end groups.[15] The authors conclude that dendrimers, composed of flexible units, have a compact structure where the density is at its maximum at the center.

SANS investigations of PPI dendrimers in dilute solutions reported by Scherrenberg et al.[16] and Rietveld et al.[17] showed the $M^{1/3}$ behavior of the size of dendrimers with molar mass. This relationship proves to be independent of the character of the end group and the solvent used and is indicative of a compact (space-filling) structure with a fractal dimensionality of approximately 3 in conflict with theoretical results predicted by de Gennes and Hervet[18] and Lescanec and Muthukumar.[19] The first theoretical approach based on ideal radial growth behavior and a modified version of Edwards' method of self-consistent fields[20] revealed that there exists a limiting size for dendrimer molecules, and their density should increase towards their periphery (dense shell model). Uppuluei et al.[21] proposed a similar structure with a dense shell in order to account for the experimental rheological data. In contrast, a numerical approach revealed a dense core-type structure for these molecules with a substantial amount of back folding of the monomer subunits and an increasing density towards the center of the molecules.[22] A Monte Carlo simulation of dendrimers up to the ninth generation performed by Manfield and Klushin[22] corroborated qualitatively the results presented by Lescanec and Muthukumar. The equilibrium structure of dendrimers was recently the subject of a comprehensive study by Boris and Rubinstein.[23] A self-consistent mean field model was solved numerically to verify the Flory predictions[24] and to elucidate the density profile within the dendrimer molecule. The density was found to decrease monotonically from the center of the molecule. More recent simulations suggest that the segment distribution is rather uniform.[25]

Recent SANS studies at NIST on PAMAM dendrimers show that the R_g does not change significantly when the solvent type goes from very good to very poor.[26] Also, the charging of the dendrimers with acid addition does not significantly change the size of individual dendrimers.[27] The terminal groups of a deuterium labeled dendrimer have a larger R_g than the whole dendrimer.[28] All of these results are consistent with previous SAXS results[13] which find PAMAM dendrimers having a uniform spherical structure.

A comprehensive analysis was carried out for polyorganosiloxane dendrimers by Rebrov et al.[29] Their molecular dynamics simulations show that these dendrimer molecules have the shape of an ellipsoid of revolution 1 : 1 : 1.15 and a homogeneous distribution of density. These results correlate well with the SAXS data. The average density of dendrimer is 1.0 g/cm^3 consistent with the experimental value of 1.05 g/cm^3 for the density of polyorganosiloxane in bulk. In conclusion, the internal structure of dendrimers continues to be a matter of debate despite a decade of intense research.

Ramzi et al.[30] detected another difficulty in the interpretation of the dependence of structural parameters of dendrimers. They used SANS for the structural investigation of amine terminated PPI dendrimer solutions as a

function of concentration and acidity. It was found that the scattering intensity at $Q \rightarrow 0$ decreases progressively by increasing the concentration due to the interdendrimer correlations. They state that PPI dendrimers appear to behave as soft molecules with possible intermolecular interpenetration at higher concentrations. They also state that when the dendrimer molecules are charged by adding acid (HCl), the electrostatic repulsion dominates and the molecules tend to stretch and to behave as hard particles. These coulombic interactions can be screened again by adding an excess of acid or salt (NaCl). For the time being no clear explanation could be given for the empirical scaling relation of the interference peak position, Q_{max}, upon increasing dendrimer concentration, $Q_{max} \propto \phi^{0.55}$. More recent studies, however, have shown that dendrimers do not interpenetrate each other when forced together at high concentration and shrink in size rather than interpenetrate one another.[31, 32]

A SAXS study on highly diluted solutions of poly(benzyl ether) dendrimers was carried out by Kleppinger et al.[33] who obtained the form factor contribution of the uncorrelated macromolecules revealing a rather dense globular structure without any evidence for density differences between core and shell. The distance distribution function $P(r)$, calculated from the scattering data, appears to be rather symmetric with a slight tail towards r-values higher than twice the molecular radius of the corresponding homogeneous sphere. The suppression of the maxima in the reciprocal space data points to a slight anisotropy of molecular shape.

The second important area of structural investigations of charged dendritic structures is the characterization of polymer systems with dendrimers as host (or guest) molecules. The stoichiometry of the complexes, formed between dendrimers and other polymers, is very sensitive to the components and the external experimental conditions (type of polyelectrolyte, concentration, pH, etc.). This field of research is hardly explored and one should mention the work of Amis et al.[34] who investigated interpenetrating networks of dendrimers and polymers by SANS and state that dendrimers appear as "microgels" and "segments of macrogels".

Recently, dendritic polymers have been used as soluble templates/unimolecular reactors from which nano-clusters of inorganic compounds or metals can be synthesized. A model system of PAMAM dendrimer-copper sulfide nanocomposites was studied in various stages of its formation using a combination of SAXS and SANS.[35] There is evidence of aggregation in the nanocomposite system, which suggests that the stable form of the dendrimer/CuS hybrid species in solution is supermolecular clusters containing more than 50 individual dendrimer/copper sulfide particles.

In this paper a SANS study is presented of the relationship between the chemistry and structure of different dendrimers based on benzyl ether monomers including the effects of chemical structure, shell groups and solvent.

Experimental Part

Materials

The dendrimers were synthesized via a convergent approach using preformed building blocks (wedges or dendrons) that are coupled to the final core in the last step of synthesis as recently reported.[36–39] The molar masses of these dendrimers were determined by either MALDI-TOF (samples 101b and 150a) or by ES MS (samples 150b, 124 and 134) as described in references.[33, 39] Two-dimensional pictures of the resultant dendrimer structures are shown schematically in Figure 1–3. Highly diluted dendrimer solutions with a concentration of 1 wt.-% were prepared by mixing appropriate amounts of the compounds into HPLC-grade deuterated tetrahydrofuran (THF) or toluene. These moderately polar and non-polar solvents have nearly the same solubility parameters of $\delta = 20.3$ $(J/cm^3)^{1/2}$ (THF) and $\delta = 18.3$ $(J/cm^3)^{1/2}$ (toluene).[40] The neutron scattering length densities ρ_{sol} of deuterated solvents used were 6.36×10^{10} cm^{-2} (THF) and 5.66×10^{10} cm^{-2} (toluene).

SANS Measurements

The small-angle neutron scattering measurements (SANS) were carried out using the 8m SANS facility at the National Institute of Standards and Technology Center for Neutron Research. The scattering vectors used, defined as $|\mathbf{q}| = q = 4\pi \sin\theta/\lambda$, vary between 0.01 and 0.15 $Å^{-1}$ (λ is wavelength of incident neutron beam, 2θ is the scattering angle). The incident wavelength was 8 Å with $\Delta\lambda/\lambda = 25\%$.

The radially averaged scattering patterns were corrected for absorption, solvent scattering and instrumental background and converted into an elastic scattering cross-section (absolute intensity scale) $d\Sigma/d\Omega(q)$ using water as a secondary standard.[41] The radius of gyration R_g was calculated by applying the Guinier approximation[42] and using the Levenberg-Marquardt non-linear least-squares curve fitting algorithm as implemented in Microcal Origin (version 5.0, Microcal Software, Inc., Northampton, USA).[a] The uncertainties are calculated as the estimated standard deviation of the mean, and the total combined uncertainty is not given since comparisons are made with data obtained under the same conditions. In cases where the limits are smaller than the plotted symbols, the limits are left out for clarity. In data plots with uncertainties larger than the symbols, representative confidence limits are plotted at appropriate places. Fits of the scattering data are made by a least squares fit of the data giving an average and a standard deviation to the fit, this is true for fit values such as radius of gyration and exponents.

[a] Certain commercial materials and equipment are identified in this paper in order to specify adequately the experimental procedure. In no case does such identification imply recommendation by the National Institute of Standards and Technology nor does it imply that the material or equipment identified is necessarily the best available for this purpose.

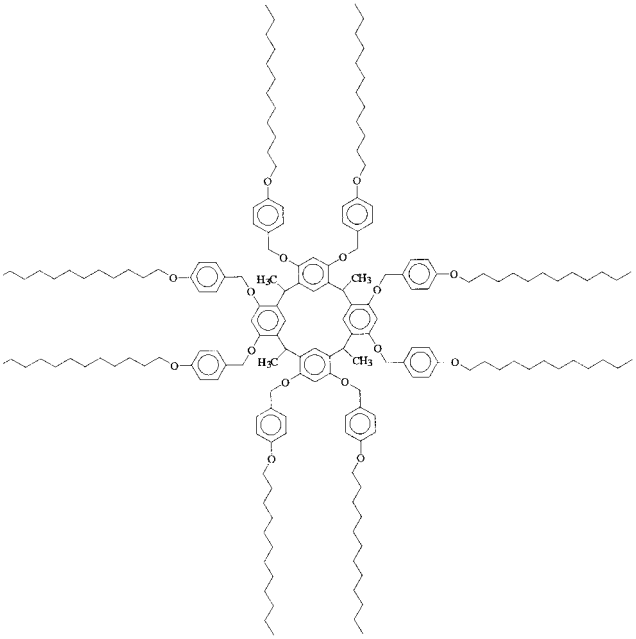

Figure 1. Schematic structure of 101b dendrimer in a two dimensional representation.

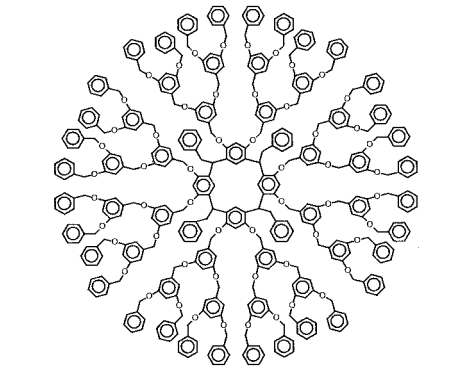

a

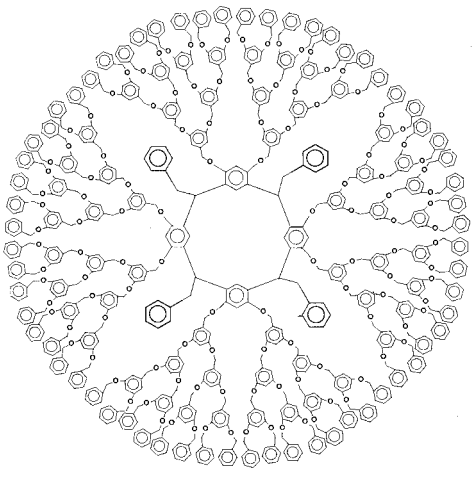

b

Figure 2. A two dimensional representation of dendritic structure for the second (a) and third (b) generation of 150 samples ([G2] and [G3] resorcinarene, respectively).

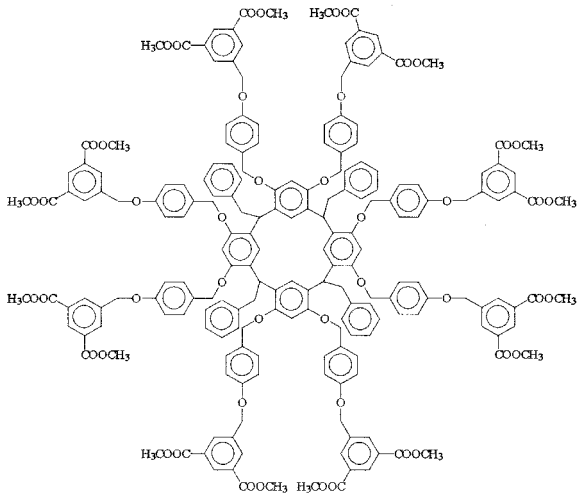

a

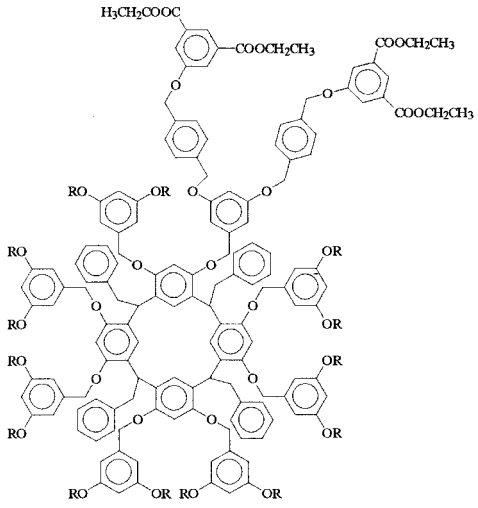

b

Figure 3. Schematic representation of molecular structure of 124 (a) and 134 sample (b).

Results and Discussion

Figure 4–6 show the scattering curves from the poly(benzyl ether) dendrimers in THF and toluene solutions. For a quantitative evaluation, SANS data were analyzed by the classical Guinier approximation in order to determine the radius of gyration R_g (Equation (1)):

$$\frac{d\Sigma}{d\Omega}(q) = \frac{d\Sigma}{d\Omega}(0) \cdot \exp\left(-\frac{q^2 R_g^2}{3}\right) \qquad (1)$$

where $d\Sigma/d\Omega(0)$ is the scattering intensity at zero angle ($q = 0$). The parameters $d\Sigma/d\Omega(0)$ and R_g were obtained by linear fitting of the experimental curves in the representation $\ln(d\Sigma/d\Omega(q))$ vs. q^2 in the Guinier regime

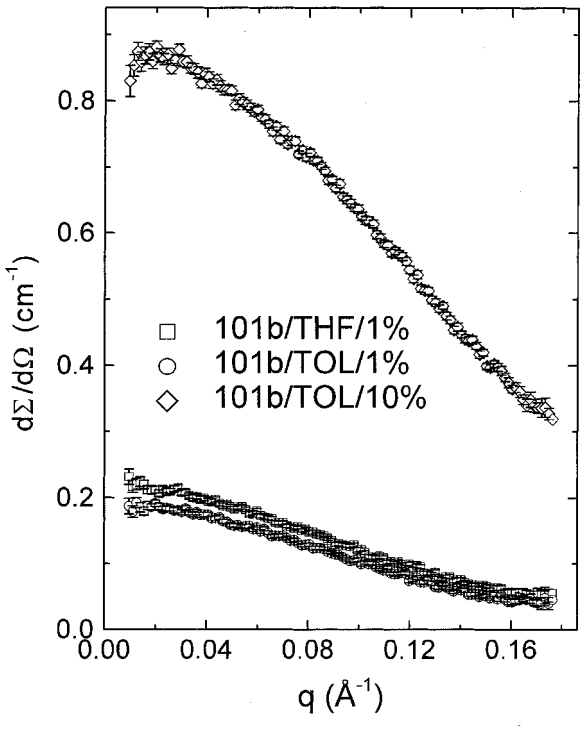

Figure 4. SANS curves for the 101b dendrimers in THF (1 wt.-%) and toluene (1 wt.-% and 10 wt.-%).

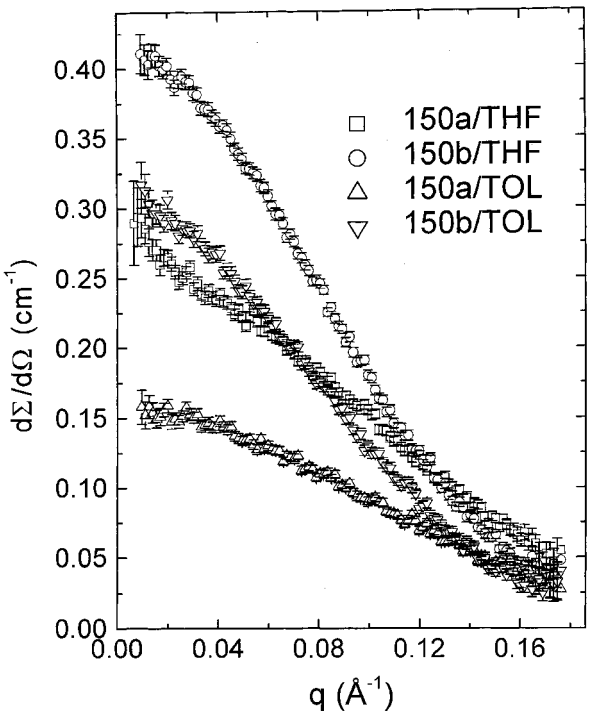

Figure 5. SANS curves of 1 wt.-% solutions of the 150a and 150b dendrimers in THF and toluene.

($qR_g < 1$) with uncertainties being one standard deviation from the goodness of the fit. The q-range of fitting was 0.01 Å^{-1} < q < 0.15 Å^{-1}. The Guinier representation of the

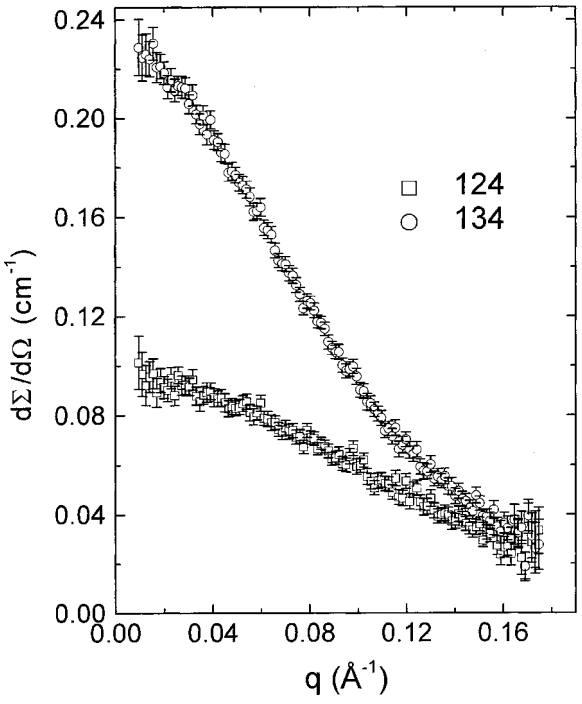

Figure 6. SANS curves of 1 wt.-% solutions of 124 and 134 samples in THF.

scattering intensity for these samples in the low q regime is shown in Figure 7–9.

The characteristics of the dendrimer solutions and the parameters, obtained from Equation (1) as described above, are given in Table 1. In this table the relative change of density of the dendrimer molecule, d_{dendr}/d_{150}, compared to the 150-samples, are presented as well with the subscript referring to the species measured.

These values were calculated according to the following equation (Equation (2)):

$$d_{dendr}/d_{150} = (M_{dendr}M_{150})(R_{g,150}/R_{g,dendr})^3 \quad (2)$$

where $R_{g,dendr}$ is the experimentally determined radius of gyration of the dendrimer molecule, and $R_{g,150}$ is the radius of gyration of the 150-sample, and M_X is the molecular mass of the dendrimer X. This value was determined from the linear fitting of the dependence of ln R_g vs. ln M for the 150-samples in THF solutions. The relationship between the radii of gyration for the samples of type 150 at various values of molecular mass were evaluated according to the Equation (3):

$$\ln R_g = -2.654 + 0.331 \cdot \ln M \ (R_g \text{ in nm}) \quad (3)$$

The scaling dependence $R_g \propto M^{0.33}$ is in line with a recent molecular dynamics study of Murat and Grest.[25] On the basis of molecular dynamics simulations, under varying solvent conditions, these authors predict a compact (space-filling) structure under all solvent conditions,

Table 1. The characteristics of the poly(benzyl ether) dendrimers.[a)]

Sample code	Content	M	Solvent	C / wt.-%	$d\Sigma/d\Omega(0)$ / cm^{-1}	Radius of gyration / Å	Relative change of density of dendrimer molecule
101b	$C_{184}H_{272}O_{16}$	2736	THF	1	0.215	13.0	0.40
101b			Toluene	1	0.189	13.4	0.34
101b			Toluene	10	0.883	10.1	0.81
150a	$C_{448}H_{384}O_{56}$	6656	Toluene	1	0.156	12.7	1.0
150a			THF	1	0.221	12.7	1.0
150b	$C_{896}H_{768}O_{120}$	13440	Toluene	1	0.301	16.0	1.0
150b			THF	1	0.414	15.9	1.0
124	$C_{200}H_{176}O_{48}$	3344	THF	1	0.0945	11.8	0.62
134	$C_{432}H_{400}O_{104}$	6888	THF	1	0.222	16.4	0.41

[a)] The uncertainty of concentrations is mass fraction 0.01% from previous experience, of R_g is ± 0.1 Å from the goodness of the fit, of $d\Sigma/d\Omega(0)$ is 0.004 from the goodness of the fit, of density is typically ±0.05. M is the theoretical value in units of g/mol.

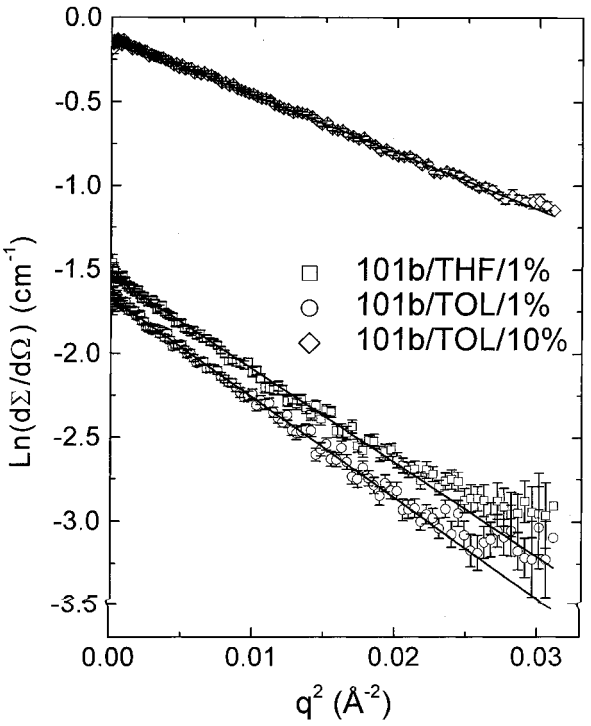

Figure 7. Guinier representation ($\ln(d\Sigma/d\Omega(q))$ vs. q^2) of the scattering intensity from 1 wt.-% and 10 wt.-% solutions of 101b dendrimer in toluene and 1 wt.-% solution of 101b dendrimer in THF. The solid lines correspond to the best fits of Equation (1) to the experimental data with the parameters listed in Table 1.

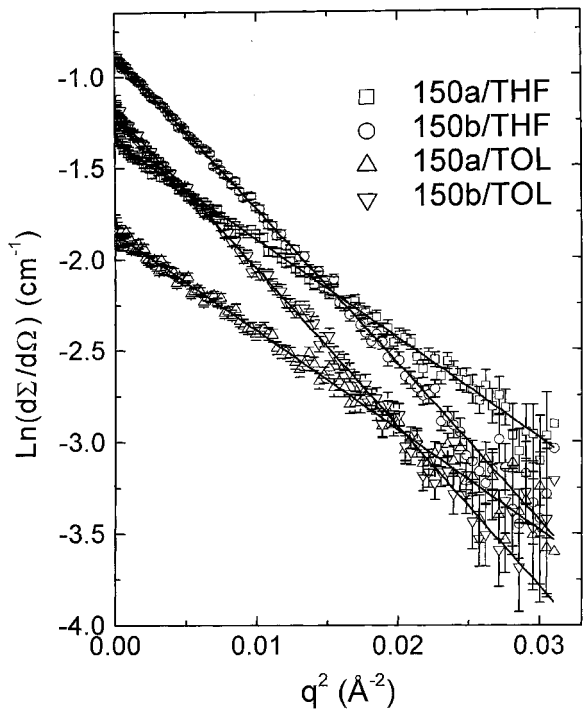

Figure 8. Guinier representation of SANS data for 1 wt.-% solutions of the 150a and 150b dendrimers in THF and toluene.

with the radius of gyration scaling with the number of monomers N as $R_g \sim N^{1/3}$.

The dependencies of the size of dendrimer molecules on their molar mass, obtained by SANS and SAXS for different dendritic systems, are presented in Figure 10 in double logarithmic scale. Also, the scaling dependence $R_g \sim M^{1/3}$ is shown for comparison. It is obvious that all of the experimental data are in good agreement with this scaling law. This shows that different dendritic systems all have a homogeneous and dense molecular structure, therefore, the compact packing of polymeric chains in such systems is a common principle of their structural organization. The conclusion of the scaling dependence as $R_g \sim M^{1/3}$ is based on the analysis of a considerable amount of data obtained on systems that are chemically quite different. The SANS results of this work do not resolve any secondary form factor maxima that have been seen for other dendrimers.[13] This can be due to either polydispersity or lack of instrumental resolution.

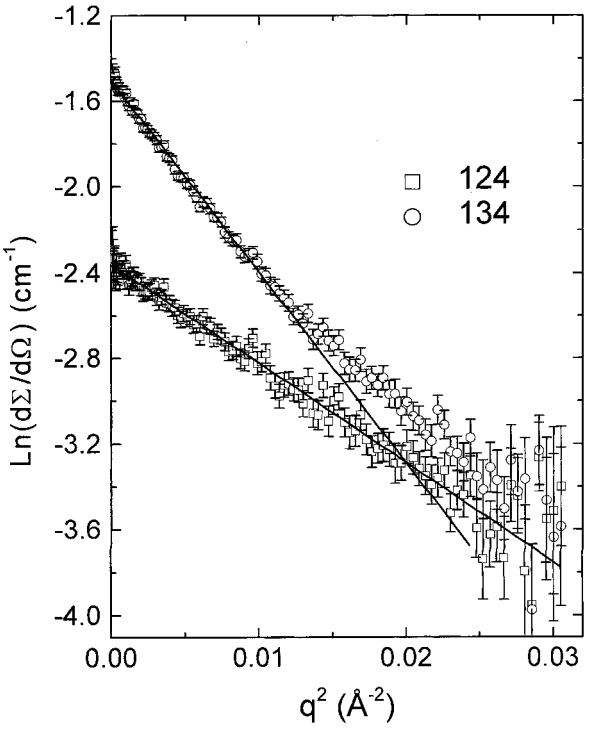

Figure 9. Guinier representation of SANS data for the 1 wt.-% solutions of 124 and 134 samples in THF.

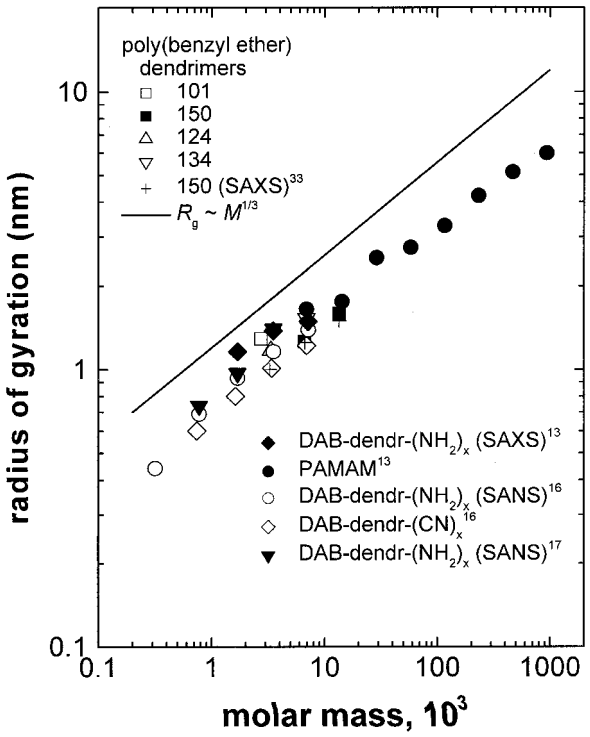

Figure 10. The dependence of the radius of gyration obtained by SANS and SAXS methods for the different dendrimers on their molecular mass, in log-log representation. The solid line represents the scaling behavior $R_g \sim M^{1/3}$.

The data in Table 1 clearly show that changing the solvent from THF to toluene causes no changes in the structural characteristics of the pure poly(benzyl ether) dendrimers of second and third generation (150a and 150b samples); the radii of gyration in both solvents are identical within the experimental uncertainty. However, the radius of gyration of the 101b sample is slightly larger in toluene (R_g = 13.4 Å) than in THF (R_g = 13.0 Å), with the difference being near the uncertainty limits of the measurements. However, a slight change may be due to the differences in the architecture of the dendrimer molecules of the 101b samples compared to the 150 samples, as can be seen from their schematic representation in Figure 1 and 3. The molecular structure of the 150 dendrimers is more compact without any distinct end parts that could cause a dependence of the structural characteristics of the dendrimer molecule on small changes in its surrounding resulting from a change of solvent. The 101b dendrimer has eight linear hydrocarbon end chains originating from the central benzyl ether core. The conformation of these chains (and hence, the size of the whole molecule) essentially depends on the type of environment. Changing the solvent from the non-polar toluene to the polar THF with practically the same solubility parameters could possibly involve a contraction of the aliphatic part to the central core of the dendrimer molecule and accordingly a decrease of the radius of gyration.

The data of the relative density changes of the different dendrimer molecules (see the last column of Table 1) clearly show the relationship between molecular design of the dendrimer and the degree of its internal packing (space filling density). Dendrimers with homogeneous density profile (such as the 150a and 150b samples) have the more compact conformation resulting from a dense packing of the polymer chains in contrast to the more open molecular architecture of the 101b, 124 and 134 samples with the less dense supermolecular structure in solution (see, for example, the data of relative change of density of dendrimer molecule given in Table 1). The dendrimer density decreases from 150a and 150b samples to 124 and 134, and finally to the 101b sample.

From our SANS data another characteristic feature of the dendrimers can be measured, i.e. the "contraction" of the polymer molecule as the concentration of the solution increases. The fit of the radius of gyration of 101b dendrimer molecule decreases from 13.4 Å to 10.1 Å in going from 1 wt.-% to 10 wt.-% solution. In this case the calculated internal density of the polymer packing increases two times, as can be seen in Table 1. This observation is consistent with similar results obtained for PPI dendrimers by Topp et al.[31,32] and Ramzi et al.[30] who attribute the reduction in R_g on concentration to virial effects. In our case of 101b dendrimers the mass fraction of 10 wt.-% is also close to the overlap concentration of 21 wt.-%, which was estimated according to $M/((4\pi/3)R^3 N_A d)$ assuming spherical particles. Here, M is the

Table 2. Neutron scattering length densities ρ_{dendr} and $\langle\rho\rangle$ for the poly(benzyl ether) dendrimer solutions and the fraction of solvent ϕ_{sol} in dendrimer molecule.[a)]

Sample code	Content	M	Solvent	C / wt.-%	Σb_1 / 10^{-12} cm	ρ_{dendr} / 10^{10} cm^{-2}	$\langle\rho\rangle$ / 10^{10} cm^{-2}	ϕ_{sol} / % v/v
101 b	$C_{184}H_{272}O_{16}$	2736	THF	1	29.9	0.66	3.07	42.3
101 b			Toluene	1			2.71	41.0
101 b			Toluene	10			2.58	38.4
150 a	$C_{448}H_{384}O_{56}$	6656	Toluene	1	187	1.69	2.75	26.7
150 a			THF	1			2.90	25.9
150 b	$C_{896}H_{768}O_{120}$	13440	Toluene	1	378	1.69	2.81	28.2
150 b			THF	1			2.98	27.6
124	$C_{200}H_{176}O_{48}$	3344	THF	1	95	1.71	3.83	45.5
134	$C_{432}H_{400}O_{104}$	6888	THF	1	198	1.73	4.00	49.0

[a)] The uncertainty of concentrations is mass fraction 0.01% from previous experience, of $\langle\rho\rangle$ is $\pm 0.05 \cdot 10^{10}$ cm^{-2}, and ϕ_{sol} is ±2%. The neutron cross sections and densities are calculated. M is the theoretical value in units of g/mol.

molar mass of the dendrimer, N_A is the Avogadro number, $R = (5/3)^{1/2} R_g$ is the radius of the dendrimer, and the dendrimer density d was approximated as 1 g/cm^3. Previous results for PAMAM dendrimers[31, 32] only see shrinkage at concentrations greater than the overlap concentration. Therefore, the decrease of R_g is probably only apparent since the interparticle effects decrease the low Q scattering but do not necessarily change the actual dendrimer size.

A more detailed analysis of the structural parameters obtained from SANS measurements, i.e. the values of $d\Sigma/d\Omega(0)$ and R_g, allows one to determine the mean scattering length densities $\langle\rho\rangle$ of the scattering heterogeneities in the dendrimer solutions, as calculated by the following equation (Equation (4)):

$$\langle\rho\rangle = \left| \frac{33.3}{R_g} \cdot \sqrt{\frac{d\Sigma/d\Omega(0)}{\phi R_g}} - \rho_{sol} \right| \quad (4)$$

where $d\Sigma/d\Omega(0)$ is obtained by extrapolation of the coherent scattering intensity to zero angle (the experimental intensities were converted to absolute differential scattering cross sections per unit sample volume as has been described earlier), ϕ is the volume fraction of dendrimer in solution (in the present case this value is roughly equal to the concentration of the dendrimer solution), R_g is the measured radius of gyration of the dendrimer (in Å) and ρ_{sol} is the scattering length density of the solvent. Equation (4) assumes spherical symmetry of the scattering heterogeneities in dendrimer solutions. In this case their volume is $V = (4/3)\pi R^3$, R being the radius of a sphere and $R_g^2 = (3/5)R^2$.

From these data one calculates the fraction of solvent in the dendrimer molecule by Equation (5):

$$\phi_{sol} = \frac{\langle\rho\rangle - \rho_{dendr}}{\rho_{sol} - \rho_{dendr}} \quad (5)$$

where the scattering length densities, ρ_{dendr}, were calculated from the chemical composition of the dendrimer according to Equation (6):

$$\rho_{dendr} = \sum_i b_i \cdot d \cdot N_A / M \quad (6)$$

b_i is the coherent neutron scattering length for the ith atom (the summation is carried out over all the atoms), N_A is Avogadro's number, M is molar mass of the dendrimer, d is the density of the substance (the value of the density of the dendrimer is assumed to be that of the density of the solid dendrimer).

The calculated values of ρ_{dendr}, $\langle\rho\rangle$ and ϕ_{sol} are shown in Table 2. On the whole, these results are in line with the structural characteristics reported in Table 1. From these data additional information is obtained about the amount of solvent in the dendrimer molecules. The relative change of the neutron scattering density of the dendrimer molecules follows the trend of the fraction of solvent, ϕ_{sol}, in the dendrimer molecule; the lower the relative density the larger solvent content inside the dendritic structure and vice versa. As one can see from Table 2, the value ϕ_{sol} has the range 26% to 28% in the case of the dense, highly branched architecture of 150 a and 150 b dendrimers, and ranges from 41% to 45% for dendrimers with a more open dendritic structure (101b, 124 and 134 samples).

Conclusions

The results demonstrate the relationship between the topology of the dendritic molecules and their size and internal composition. The architecture of dendrimer molecules influences the sensitivity of the structural parameters of poly(benzyl ether) dendrimers to concentration or solvent characteristics. These results are important to future investigations of the synthesis of dendritic systems with appropriate designs in order to obtain dendrimers with controlled properties.

The poly(benzyl ether) dendrimers have an homogeneous density profile. The size of these dendritic molecules increases as $M^{1/3}$, which is indicative for a compact structure. A comparison of published results from different dendritic systems allows the conclusion that the scaling law and the structural organization is constant over a wide range of chemically different dendrimers.

Acknowledgement: This work has been supported by the *University of Leuven*, the *Ministerie voor Wetenschapsbeleid*, *FWO-Vlaanderen* and *INTAS*. G.E., R.K., N.M. and B.F. are grateful to the *Research Council of K.U. Leuven* and the *IWT*, respectively for a research fellowship. This material is based upon work supported in part by the *U.S. Army Research Office* under contract number 35109-CH.

Received: March 13, 2000
Revised: September 11, 2000

[1] O. A. Matthews, A. N. Shipway, J. F. Stoddart, *Prog. Polym. Sci.* **1998**, *23*, 1.
[2] J. M. J. Fréchet, *Science* **1994**, *263*, 1710.
[3] C. J. Hawker, J. M. J. Fréchet, *J. Chem. Soc., Perkin Trans. 1* **1992**, 2459.
[4] K. L.Wooley, J. M. J. Fréchet, C.J. Hawker, *Polymer* **1994**, *35*, 4489.
[5] E. Buhleier, W. Wehner, F. Vögtle, *Synthesis* **1978**, 155.
[6] J. F. G. A. Jansen, E. M. M. de Brabander-van den Berg, E. W. Meijer, *Science* **1994**, *266*, 1226.
[7] P. Welch, M. Muthukumar, *Macromolecules* **1998**, *31*, 5892.
[8] R. Roy, *Polym. News* **1996**, *21*, 226.
[9] T. K. Lindhorst, *Nachr. Chem. Tech. Lab.* **1996**, *44*, 1073.
[10] R. M. Briber, B. J. Bauer, B. Hammouda, D. A. Tomalia, *ACS PMSE Prepr.* **1992**, *67*, 430**.**
[11] B. J. Bauer, R. M. Briber, B. Hammouda, D. A. Tomalia, *ACS PMSE Prepr.* **1992**, *66*, 704.
[12] B. Stark, B. Stühn, H. Frey, C. Lach, K. Lorenz, B. Frick, *Macromolecules* **1998**, *31*, 5415.
[13] T. J. Prosa, B. J. Bauer, E. J. Amis, D. A. Tomalia, R. Scherrenberg, *J. Polym. Sci., Part B: Polym. Phys.* **1997**, *35*, 2913.
[14] A. Ramzi, B. J. Bauer, R. Scherrenberg, P. Froehling, J. Joosten, E. J. Amis, *Macromolecules* **1999**, *32*, 4983.
[15] D. Pötschke, M. Ballauff, P. Lindner, M. Fischer, F. Vögtle, *Macromolecules* **1999**, *32*, 4079.
[16] R. Scherrenberg, B. Coussens, P. van Vliet, G. Edouard, J. Brackman, E. M. M. de Brabander, K. Mortensen, *Macromolecules* **1998**, *31*, 456.
[17] I. B. Rietveld, J. A. M. Smit, *Macromolecules* **1999**, *32*, 4608.
[18] P.-G. de Gennes, H. Hervet, *J. Phys.* (*Paris*) **1983**, *44*, L351.
[19] R. L. Lescanec, M. Muthukumar, *Macromolecules* **1990**, *23*, 2280.
[20] S. F. Edwards, *Proc. Phys. Soc. London* **1965**, *85*, 613.
[21] S. Uppuluri, S. E. Keinath, D. A. Tomalia, P. R. Dvornic, *Macromolecules* **1998**, *31*, 4498.
[22] M. L. Mansfield, L. L. Klushin, *Macromolecules* **1993**, *26*, 4262.
[23] D. Boris, M. Rubinshtein, *Macromolecules* **1996**, *29*, 7251.
[24] P. J. Flory, "*Principles of Polymer Chemistry*", Cornell University Press, Ithaca, NY, 1953.
[25] M. Murat, G. S. Grest, *Macromolecules* **1996**, *29*, 1278.
[26] A. Topp, B. J. Bauer, D. A. Tomalia, E. J. Amis, *Macromolecules* **1999**, *32*, 7232.
[27] G. Nisato, R. Ivkov, E. J. Amis *Macromolecules* **1999**, *32*, 5895.
[28] A. Topp, B. J. Bauer, J. W. Klimash, R. Spindler, D. A. Tomalia, E. J. Amis, *Macromolecules* **1999**, *32*, 7226.
[29] A. V. Rebrov, M. A. Fadeev, A. N. Ozerin, *Dokl. Chem.* **1998**, *1–3*, 88.
[30] A. Ramzi, R. Scherrenberg, J. Brackman, J. Joosten, K. Mortensen, *Macromolecules* **1998**, *31*, 1621.
[31] T. J. Prosa, B. J. Bauer, A. Topp, E. J. Amis, R. Scherrenberg, *ACS PMSE Prepr.* **1998**, *79*, 307.
[32] A. Topp, B. J. Bauer, T. J. Prosa, R. Scherrenberg, E. J. Amis, *Macromolecules* **1999**, *32*, 8923.
[33] R. Kleppinger, H. Reynaers, K. Desmedt, B. Forier, W. Dehaen, M. Koch, P. Verhaert, *Macromol. Rapid Commun.* **1998**, *19*, 111.
[34] E. J. Amis, B. J. Bauer, A. T. C. Jackson, T. J. Prosa, Program and abstracts of 14th Polymer Networks Group International Conference "Polymer Networks 98", Trondheim, Norway, June 28–July 3, 1998, P18.
[35] N. C. Beck Tan, L. Balogh, S. F. Trevino, D. A. Tomalia, J. S. Lin, *Polymer* **1999**, *40*, 2537.
[36] C. J. Hawker, J. M. J. Fréchet, *J. Chem. Soc., Chem. Commun.* **1990**, 1010.
[37] C. J. Hawker, J. M. J. Fréchet, *J. Am. Chem. Soc.* **1990**, *112*, 7638.
[38] G. L'abbé, B. Forier, W. Dehaen, *J. Chem. Soc., Chem. Commun.* **1996**, 2143.
[39] B. Forier, W. Dehaen, *Tetrahedron* **1999**, *55*, 9829.
[40] E. A. Collins, J. Bareš, F. W. Billmeyer, "*Experiments in polymer science*", Wiley, New York 1973.
[41] National Institute of Standards and Technology – Center for Neutron Research: NG3 and NG7 #0-meter SANS Instruments: Data Acquisition Manual and SANS Data Reduction and Imaging Software, Gaithersburg, 1998.
[42] A. Guinier, G. Fournet, "*Small-angle scattering of X-rays*", Wiley, New York 1955.